

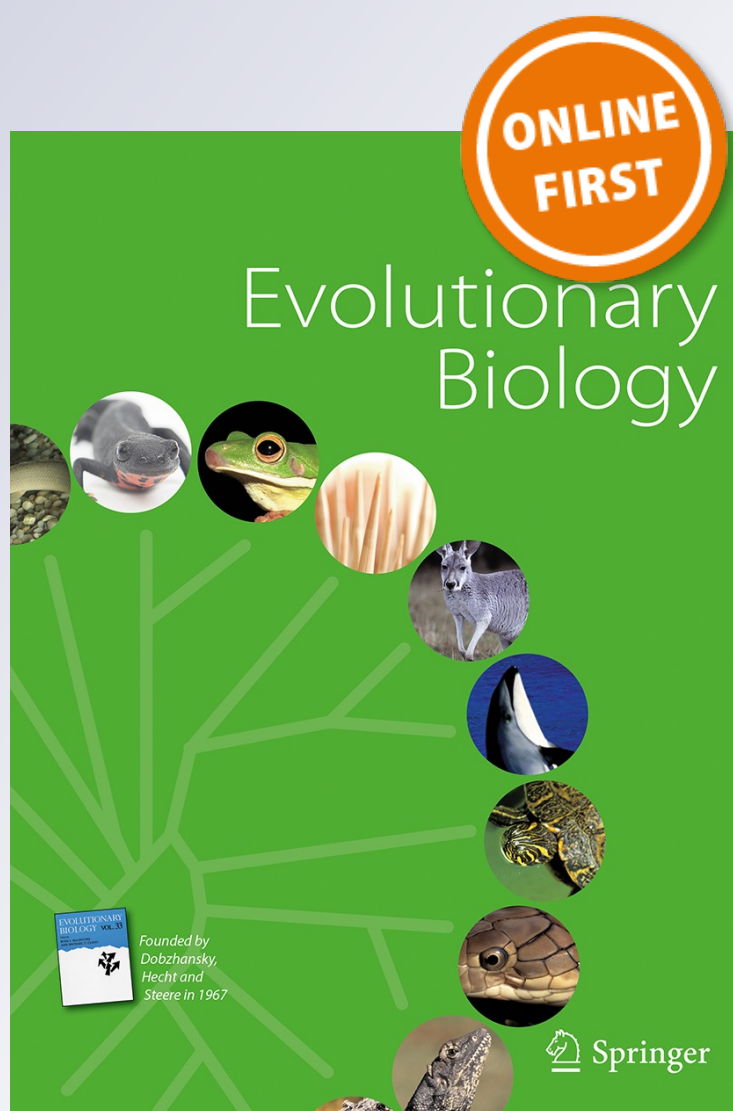
# *The Role of Evolutionary Integration in the Morphological Evolution of the Skull of Caviomorph Rodents (Rodentia: Hystricomorpha)*

**Alicia Álvarez, S. Ivan Perez & Diego  
H. Verzi**

**Evolutionary Biology**  
Evolutionary Biology

ISSN 0071-3260

Evol Biol  
DOI 10.1007/s11692-015-9326-7



 Springer

**Your article is protected by copyright and all rights are held exclusively by Springer Science +Business Media New York. This e-offprint is for personal use only and shall not be self-archived in electronic repositories. If you wish to self-archive your article, please use the accepted manuscript version for posting on your own website. You may further deposit the accepted manuscript version in any repository, provided it is only made publicly available 12 months after official publication or later and provided acknowledgement is given to the original source of publication and a link is inserted to the published article on Springer's website. The link must be accompanied by the following text: "The final publication is available at [link.springer.com](http://link.springer.com)".**

# The Role of Evolutionary Integration in the Morphological Evolution of the Skull of Caviomorph Rodents (Rodentia: Hystricomorpha)

Alicia Álvarez<sup>1,2,5</sup> · S. Ivan Perez<sup>2,3</sup> · Diego H. Verzi<sup>2,4</sup>

Received: 19 December 2014 / Accepted: 11 May 2015  
© Springer Science+Business Media New York 2015

**Abstract** The mammalian cranium is a complex structure composed by three partially independent modules: face, cranial base and cranial vault. At the same time, it interacts with the mandible by sharing the masticatory function. Since these units develop and work together, their function and evolution may occur through correlated changes. Here, we assessed the patterns of evolutionary shape variation and covariation (i.e. integration) of cranial modules and mandible among the highly ecomorphologically diverse caviomorph rodents, and the potential evolutionary consequences on the morphological evolution of this clade. Three-dimensional geometric morphometrics was used to describe cranio-mandibular shape. The phylogenetic signal and evolutionary allometric component of morphometric variables were analyzed; in addition, evolutionary covariation among cranial modules and mandible was assessed using phylogenetic comparative methods. Significant phylogenetic signal and evolutionary allometry were detected. Large covariance

values, involving coordinated breadth increase as the main shape change, were recorded between cranial vault and base, followed by cranial vault and face, and face and mandible. Since the basicranium may be the main cranial integrator, the overall widening of the cranial base, derived from the enlargement of the auditory bullae, could be influencing the integrated evolution of skull. In caviomorphs, the cranio-mandibular morphological evolution would be the outcome of a tight covariation among the modular units, and this could be driven by several factors such as allometry and specializations to environmental niches.

**Keywords** Caviomorph rodents · Evolutionary allometry · Geometric morphometrics · Morphological integration

## Introduction

The mammalian cranium is one of the most studied biological structures in the context of analyses of morphological integration (e.g. Marroig and Cheverud 2001; Ackermann and Cheverud 2004; Goswami 2006; Cardini and Elton 2008; Mitteroecker and Bookstein 2008; Porto et al. 2009; Goswami and Polly 2010; Koyabu et al. 2014). It is a complex structure which bears numerous capsules that surround and protect the brain and sense organs (Lieberman 2011), and it is part of the masticatory complex (Emerson and Bramble 1993). The phenotypic inter-dependence of the components of the cranium that arises from the conjoint development and function is referred as morphological integration (Willmore et al. 2007). It has been suggested that the integration of the cranium is not pervasive, and those components are structured into

✉ Alicia Álvarez  
alvarez.ali@gmail.com

<sup>1</sup> División Mastozoología, Museo Argentino de Ciencias Naturales “Bernardino Rivadavia”, Av. Ángel Gallardo 470, C1405DJR Buenos Aires, Argentina

<sup>2</sup> CONICET, Buenos Aires, Argentina

<sup>3</sup> División Antropología, Facultad de Ciencias Naturales y Museo, Universidad Nacional de La Plata, Paseo del Bosque s/n, B1900FWA La Plata, Argentina

<sup>4</sup> Sección Mastozoología, División Zoología Vertebrados, Facultad de Ciencias Naturales y Museo, Universidad Nacional de La Plata, Paseo del Bosque s/n, B1900FWA La Plata, Argentina

<sup>5</sup> Present Address: CIT-Jujuy CONICET, Instituto de Geología y Minería, Universidad Nacional de Jujuy, Av. Bolivia 1661, Y4600GNE S. S. de Jujuy, Argentina

partially independent modules: the face, the cranial base and the cranial vault (Moss and Young 1960; Cheverud 1982; Lieberman et al. 2000; Hallgrímsson et al. 2007a; Klingenberg 2013). At the same time, the cranium interacts with the mandible by sharing the masticatory function. The need for an adequate performance of the masticatory apparatus demands coordinated changes of the cranium and the mandible as they vary through development, growing, and evolution. The study of the relationships of the long-time among cranial modules and the effects of the shape changes occurred in one module on another one are of main interest in a macroevolutionary context because of the deep influence of modularity and integration on morphological evolution. At this level, evolutionary integration takes place when morphological features evolve coordinately (Cheverud 1996; Willmore et al. 2007).

According to previous studies on integration of mammalian skull, the most common pattern of variation observed among modules involves a high covariation between those units that are linked by genetic, developmental, and/or functional factors (e.g. Moss and Young 1960; Cheverud 1982; Lieberman et al. 2000; Hallgrímsson et al. 2007a, b; Mitteroecker and Bookstein 2007). Among cranial modules, the basicranium has been stated as a potential skull integrator (Lieberman et al. 2000; Hallgrímsson and Lieberman 2008; Lieberman 2011; Neaux et al. 2013), probably acting as a constraint or a driver at the evolutionary scale. Among the reasons, it is located in the center of the head, between the brain and the face, and serves as the platform on which rest the brain and neurocranium; second, it is developmentally distinctive since it ossifies endochondrally (unlike others parts of cranium that develops intramembranously) and reaches the adult size first (Lieberman et al. 2000; Lieberman 2011). Another potential integrating key factor involves allometry, which has large-scale effects on morphological variation through size variation and may affect all parts of the skull (Rosas and Bastir 2004; Klingenberg 2009, 2013). Because of this, the identification of modules should become clearer after removing the allometric size effects and thus narrowing the covariances between modules (Mitteroecker and Bookstein 2007; Klingenberg 2009).

Integration and modularity at evolutionary scale have been studied in several mammalian clades (e.g. primates, carnivorans, marsupials, soricids; Ackermann and Cheverud 2004; Goswami 2006; Marroig et al. 2009; Porto et al. 2009; Goswami and Polly 2010; Goswami et al. 2012; Cornette et al. 2013; Koyabu et al. 2014). These comparative studies support the conservation of patterns of cranial integration during mammalian evolution, which is in agreement with the detected common developmental patterns in the skull of mammals (Porto et al. 2009; Goswami et al. 2014). However, patterns of integration remain

scarcely explored among South American caviomorph rodents (see Monteiro et al. 2005; Koyabu et al. 2014). Caviomorphs represent an excellent model because they display diverse modes of life (arboreal, epigeal, semi-aquatic, fossorial, subterranean; Mares and Ojeda 1982; Elissamburu and Vizcaíno 2004) and inhabit a wide variety of habitats (Nowak 1991; Eisenberg and Redford 1999; Patton et al. 2015). Concurrently, they are morphologically diverse, with a wide range of body size (Sánchez-Villagra et al. 2003; Rinderknecht and Blanco 2008) and skeletal variation (Vassallo and Verzi 2001; Weisbecker and Schmid 2007; Candela and Picasso 2008; Morgan 2009; Álvarez et al. 2011, 2013). Previous studies regarding overall skull variation in caviomorphs (Vassallo and Verzi 2001; Monteiro et al. 2003; Perez et al. 2009; Hautier et al. 2012; Álvarez et al. 2013) coincide in detecting coordinated changes among skull features, such as the decrease of the length of the snout and tooth row, the narrowing of the cranial base, the enlargement of the tympanic bulla, the deepening of the mandibular horizontal ramus, more robust and higher coronoid and condylar processes, and the shortening of the angular process. Also, allometry was pointed out as a key dimension (among others, such as ecological factors and phylogeny; Hautier et al. 2012; Álvarez et al. 2013) to explain a large proportion of the morphological variation among caviomorphs.

Here, we assess the patterns of evolutionary shape variation and integration of the modules of the cranium (face, cranial base and vault; e.g. Bookstein et al. 2003; Hallgrímsson et al. 2007a) and the mandible among the highly eco-morphologically diverse caviomorph rodents, and discuss the effects of integration on morphological evolution. Given the seemingly widespread pattern of high covariation between cranial modules among mammals (e.g. facial and basicranial modules; Goswami 2006), it could be expected a similar pattern among caviomorph rodents. This was assessed through partial least squares analysis carried out among three-dimensional landmark coordinates datasets for each cranial module and mandible, and through the estimation of covariation parameters. For these, high values are to be expected if there is a strong association between the shape changes of each module. Moreover, if a particular module is investigated as a cause of integration, such as the cranial base, then it should show the highest values of covariation with the other modules. Finally, to assess the extent of influence of allometry on the patterns of integration observed, we carried out a partial least squares analysis of the residuals of the allometric regressions of modular shape datasets on size. In this context, the evolutionary integration detected could be the outcome of developmental constraints or drivers acting on the generation of variation or the correlated selection of different/independent traits.

## Materials and Methods

The total sample included 200 specimens belonging to 24 genera (Table 1). Only adults, defined by the presence of a functional third molar, were included in the analyses.

Forty-three and 16 three-dimensional landmarks were recorded on one side of the cranium and mandible, respectively (Fig. 1; Table 2) using a digitizer (Inmersion Microscribe G2X; Inmersion Corp., San José, California, USA). We considered the skull as divided in three modules which contain anatomic and functional information (Fig. 1): the *face* that includes premaxillary, maxillary, nasal, lacrimal and jugal bones; the *cranial vault*, comprising frontal, squamosal, parietal, and occipital bones; and the *cranial base* that includes the basioccipital and basisphenoid bones, and auditory bullae. For each cranial module and *mandible*, separate Generalized Procrustes Analyses (GPA) were carried out to obtain the consensus configuration for each genus. Then, a second series of GPA, one for each module, was performed on the mean shapes of the 24 genera in order to obtain a matrix of aligned Procrustes coordinates including all genera. These matrices were then analyzed through Principal Component Analyses (PCA) in order to explore shape variation of each module and mandible.

To analyze the allometric trends in modular shape variation, ordinary least squares regression analyses were conducted between shape (i.e. Procrustes coordinates) and

size (natural logarithm of centroid size; lnCS) of each cranial module and the mandible. Phylogenetic signal of the shape of cranial modules and the mandible was estimated using the multivariate  $K$  ( $K_{mult}$ ) statistic for the Procrustes coordinates datasets of each cranial module and mandible (Adams 2014). This statistics represents a multivariate generalization of the univariate  $K$  statistic proposed by Blomberg et al. (2003).  $K_{mult}$  provides a measure of the strength of phylogenetic signal of the data: values near 0 indicate a lack of signal and values around 1 are expected for a character evolving under the Brownian motion model; further, values  $<1$  imply that taxa resemble each other less than expected under Brownian motion and values  $>1$  imply that taxa resemble each other more than expected (Adams 2014). Significance of  $K_{mult}$  was assessed by permutation tests with 999 replications. These analyses were carried out using the package Geomorph (Adams and Otárola-Castillo 2013) for R (ver. 3.1.1; R Development Core Team 2014).

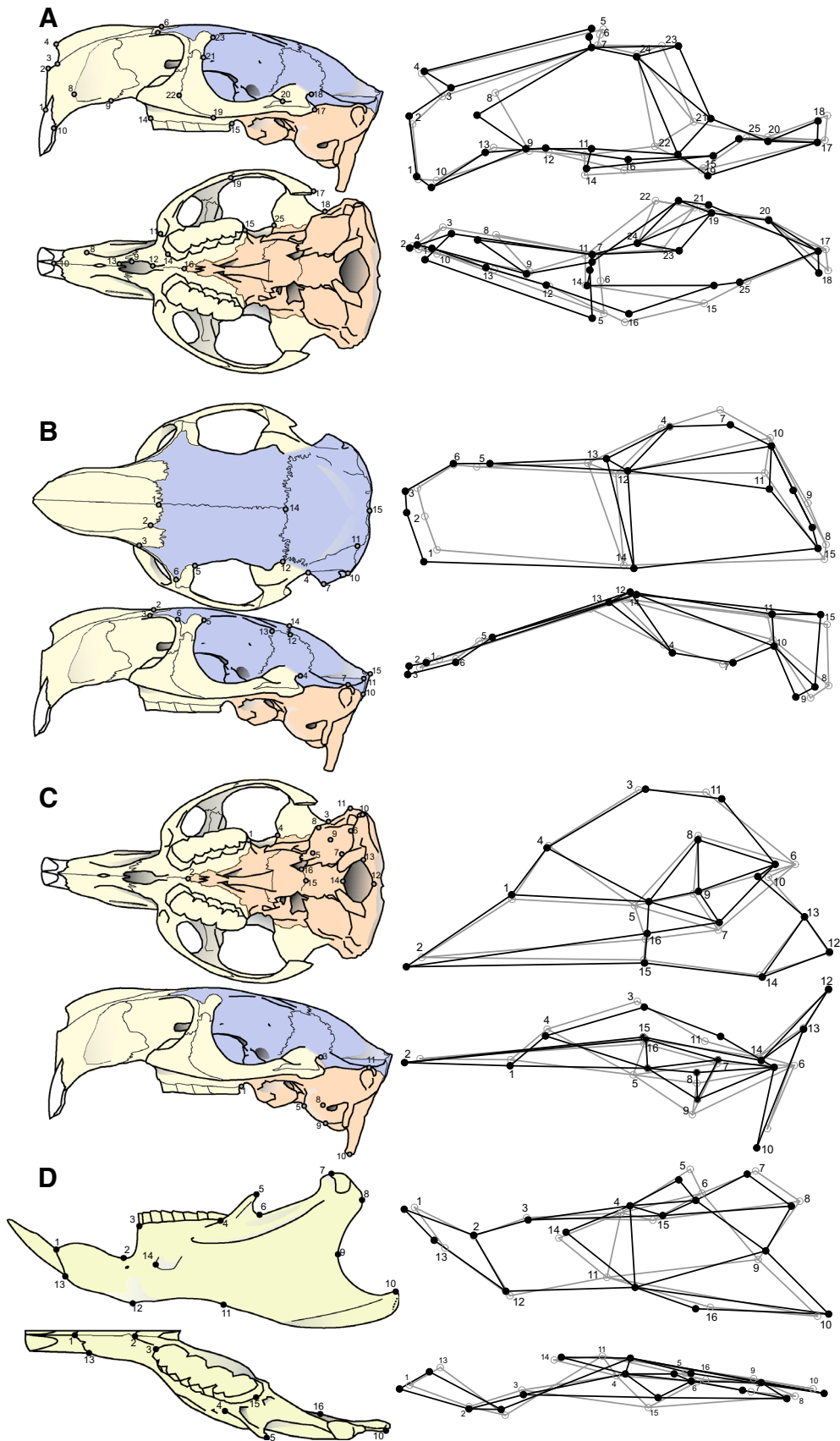
In the context of an evolutionary approach, it is necessary to take into account the expected lack of independence among samples resulting from phylogenetic structure (Felsenstein 1985). We estimated the phylogenetically independent contrasts (IC) of shape and size, as the differences (i.e. contrasts) between the values of both the Procrustes coordinates and lnCS of each pair of sister nodes of the caviomorph phylogeny considered here (the same used by Álvarez et al. 2013). To explore evolutionary shape changes we carried out a PCA on each IC shape dataset. Also, we analyzed the evolutionary allometry of each module and the mandible through multivariate regressions of IC of shape on IC of size (as in Klingenberg and Marugán-Lobón 2013).

Covariation among cranial modules and mandible was analyzed through the two-blocks partial least squares approach (2B-PLS; Rohlf and Corti 2000). This method assesses the covariation between two datasets, or blocks (e.g. the Procrustes coordinates matrices for the cranial modules and the mandible). PLS constructs linear combinations between the variables of the two blocks which give account for as much as possible of the covariation between the two original datasets (Rohlf and Corti 2000). In the context of modularity, covariation patterns can be interpreted as the presence of integration patterns among modules; the higher the covariation between two modules, the larger is the integration. For geometric morphometric data, the linear combinations of shape variables produced by the 2B-PLS analysis can be directly expressed as deformations by using thin-plate spline (Rohlf and Corti 2000). Prior to PLS analysis, the landmark configuration of each module underwent separate Procrustes fits. As a first analysis, we obtained the linear combinations between the Procrustes coordinates matrices of the three cranial

**Table 1** Studied caviomorph taxa and number of specimens examined ( $N$ )

Taxa	$N$	Taxa	$N$
<b>Cavioidea</b>		<b>Octodontoidea</b>	
<b>Caviidae</b>		<b>Abrocomidae</b>	
<i>Cavia aperea</i>	9	<i>Abrocoma cinerea</i> complex	6
<i>Galea leucoblephara</i>	9	<b>Echimyidae</b>	
<i>Microcavia australis</i>	11	<i>Myocastor coypus</i>	9
<i>Dolichotis patagonum</i>	12	<i>Proechimys guyanensis</i>	3
<i>Pediolagus salinicola</i>	4	<i>Thrichomys</i> sp.	6
<i>Hydrochoerus hydrochaeris</i>	9	<b>Octodontidae</b>	
<i>Kerodon rupestris</i>	4	<i>Aconaemys porteri</i>	3
<b>Dasyproctidae</b>		<i>Aconaemys sagei</i>	3
<i>Dasyprocta</i> sp.	16	<i>Octodon degus</i>	3
<b>Cuniculidae</b>		<i>Octodon bridgesi</i>	5
<i>Cuniculus paca</i>	8	<i>Octodontomys gliroides</i>	11
<b>Chinchilloidea</b>		<i>Octomys mimax</i>	7
<b>Chinchillidae</b>		<i>Pipanacoctomys aureus</i>	11
<i>Chinchilla</i> sp.	5	<i>Spalacopus cyanus</i>	4
<i>Lagidium viscacia</i>	10	<i>Tympanoctomys barrerae</i>	12
<i>Lagostomus maximus</i>	10	<i>Ctenomys australis</i>	1
		<i>Ctenomys talarum</i>	9

Bold indicate Superfamilies and Families included in this study



◀ **Fig. 1** Landmarks used in the present study, recorded using a Microscribe G2X digitizer. **a** Facial module (landmark 5 is dorsal), **b** cranial vault (landmarks 8 and 9 are ventral), **c** cranial base, and **d** mandible

modules and the mandible. A second set of 2B-PLS analyses was carried out on the independent contrasts of each Procrustes coordinates matrices (IC of shape). Finally, in order to assess the extent of the influence of allometry on integration patterns, a third set of 2B-PLS analyses was carried out among the independent contrasts of the residuals of the ordinary least squares regressions between cranial modules and mandible shape datasets and size. For the three analyses, and in order to quantify the strength of the overall association among cranial modules and the mandible, the RV coefficient and covariation/correlation values were estimated (Klingenberg 2009). RV parameter takes values from 0 for complete independence to 1 for total interdependence between datasets. Significance of these values was assessed by permutation tests.

Morphometric (GPA, PCA, and allometric regressions) and PLS analyses were conducted in MorphoJ software (Klingenberg 2011).

## Results

### Shape Variation of Cranial Modules and Mandible

#### Facial Module

The first two principal components explained near 48 % (PC1 27.37 %, PC2 20.55 %) of total shape variation. The distribution of genera in this morphospace followed the division into superfamilies (Fig. 2). Most members of Octodontoidea superfamily were located at positive values of PC1, those of Cavioidea, on negative values, and Chinchilloidea members were situated at intermediate values of this axis and separated toward positive values of PC2. Shape changes toward positive values of PC1 were linked to shallower and narrower rostrum, broader rostral masseteric fossa, dorsoventrally expanded zygomatic arch, lesser bizygomatic breadth, longer incisive foramina, and upper tooththrows highly convergent (Fig. 2). Shape changes toward positive values of PC2 associated to shallower rostrum, poorly dorsoventrally developed zygomatic arch, nasals with wider posterior end, and convergent upper tooththrows. The cavioid *Cuniculus* was situated at extreme negative values of PC2 because of the presence of a deep rostrum, wide and short masseteric rostral fossa, the surface of the anterior part of the zygomatic arch which is outgoin, and practically parallel upper tooththrows.

#### Cranial Vault Module

The two first axes explained 65 % (PC1 52 %, PC2 12.68 %) of total shape variation. The relative position of major caviomorph clades was roughly similar to that observed in the previous analysis (Fig. 3). Main shape changes toward positive values of PC1 involved a reduced frontal area that was caudally retracted, and a wider cranial vault which presented lesser dorso-ventral expansion (Fig. 3). Along positive values of PC2, the shape changes were related to the bending and shortening of the cranial vault.

#### Cranial Base Module

The first two principal components explained 66 % (PC1 52 %, PC2 14 %) of total shape variation. Octodontids were located through positive values of PC1, separated from the other caviomorph genera (Fig. 4); most cavioids were located at negative values of PC1, whereas chinchilloids placed within the areas occupied by cavioids (*Lagostomus* and *Lagidium*) or octodontoids (*Chinchilla*). Hypertrophied auditory bullae and a narrower cranial base were the main changes expressed toward positive values of PC1. Along PC2, only the cavioid *Hydrochoerus* was clearly separated toward positive values, mainly due to the development of the paroccipital processes.

#### Mandible

The first two principal components explained approximately 61 % of the total shape variation. A clear separation of major caviomorph clades analyzed was observed in this morphospace (Fig. 5). Octodontoids were located at positive values of PC1; most cavioids occupied negative values of this axis; the chinchilloids *Chinchilla* and *Lagidium* were situated at intermediate values whereas *Lagostomus* placed among cavioids. Main shape changes toward positive values of PC1 involved a deeper mandible, a shorter diastema, higher and wider coronoid and condylar processes, and a relatively shorter angular process with its root anteriorly and dorsally placed. Toward positive values of PC2 the main changes were mainly linked to a poorly laterally developed angular process. On the basis of the inspection of the wireframes, an association between changes in the relative positions of the landmarks that depict the angular process in the vertical plane with the variation on the horizontal plane is evidenced; that is to say, a laterally expanded angular process shows less dorsoventral development.

The ordinary least square regressions of Procrustes coordinates on lnCS showed that cranial modules and mandible display clear allometric trends which were particularly marked in the cranial base and vault (Table 3). Conversely, the mandible and the face showed the lowest percentage values of shape variation explained by size.

**Table 2** Description of cranial and mandibular landmarks used in this study

Landmark	Definition
<i>Cranium</i>	
1	Anterior lower end of premaxillary bone (on sagittal plane) (F)
2	Anterior upper end of premaxillary bone (on sagittal plane) (F)
3	Anterior end of suture between nasal and premaxillary bones (F)
4	Anterior end of the nasal bone (F)
5	Posterior end of nasal bones suture (F, V)
6	Meeting point of sutures among premaxillary, nasal, and frontal bones (F, V)
7	Meeting point of sutures among premaxillary, maxillary, and frontal bones (F, V)
8	Anterior end of the masseteric fossa of rostrum (F)
9	Junction between maxillar-premaxillar suture and lateral margin of incisive foramen (F)
10	Antero-ventral border of incisor alveolus (F)
11	Most anterior point of the area of origin of the <i>masseter superficialis</i> muscle (F)
12 and 13	Extremities of incisive foramen (anterior and posterior, respectively) (F)
14 and 15	Extremities of tooth row (anterior and posterior, respectively) (14, 15: F; 15: B)
16	Junction between maxillary and palatine bones in the sagittal plane (F, B)
17	Posterior tip of the zygomatic arch (F)
18	Postero-dorsal end of cranial glenoid fossa (F, V)
19	Ventral meeting between maxillary and jugal bones (F)
20	Dorsal meeting between jugal and squamosal bones (F)
21	Meeting between maxillary and lacrimal bones on the anterior margin of orbit (F)
22	Most anterior end of jugal bone on the lateral aspect of zygomatic arch (F)
23	Meeting between lacrimal and frontal bones on the antero-dorsal margin of orbit (F, V)
24	Meeting point of sutures among maxillary, lacrimal, and frontal bones (F, V)
25	Junction between squamosal-alisphenoid bones suture and anterior margin of glenoid fossa (B, F)
26	Anterior end of auditory bulla (B)
27	Posterior end of auditory bulla (B)
28	Most medial point of auditory bulla (B)
29	Most lateral point of auditory bulla (B)
30	Most ventral point of auditory bulla (B)
31	Tip of paroccipital process (B)
32	Most dorsal point of the external auditory meatus (B)
33	Most dorsal point of the foramen magnum (B)
34	Dorso-medial tip of occipital condyle (B)
35	Most ventral point of the foramen magnum (B)
36	Middle point of basisphenoid-presphenoid suture (B)
37	Most lateral meeting point between basisphenoid and presphenoid bones (B)
38	Meeting point of squamosal, occipital, and tympanic bones (V)
39	Meeting point of squamosal, parietal, and occipital bones (V)
40	Meeting point of squamosal, frontal, and parietal bones (V)
41	Meeting between squamosal-frontal suture and the postero-dorsal margin of orbit (V)
42	Meeting point between frontal bones suture and anterior margin of parietal bone (V)
43	Most posterior point of skull (V)
<i>Mandible</i>	
1	Antero-dorsal border of incisor alveolus
2	Extreme of diastema invagination
3 and 15	Extremities of inferior toothrow (anterior and posterior, respectively)
4	Anterior end of base of coronoid process
5	Tip of coronoid process

**Table 2** continued

Landmark	Definition
6	Maximum curvature of incisura mandibulae
7	Anterior edge of condylar process
8	Posterior-most edge of postcondyloid process
9	Maximum curvature of curve between postcondyloid process and angular process
10	Tip of angular process
11	Dorsal-most point on ventral border of mandibular corpus
12	Posterior extremity of mandibular symphysis
13	Antero-ventral border of incisor alveolus
14	Insertion of muscle masseter medialis, infraorbital portion
16	Anterior end of mandibular pterygoid crest

The modules to which landmarks were allocated are indicated (*B* cranial base, *F* face, *V* cranial vault)

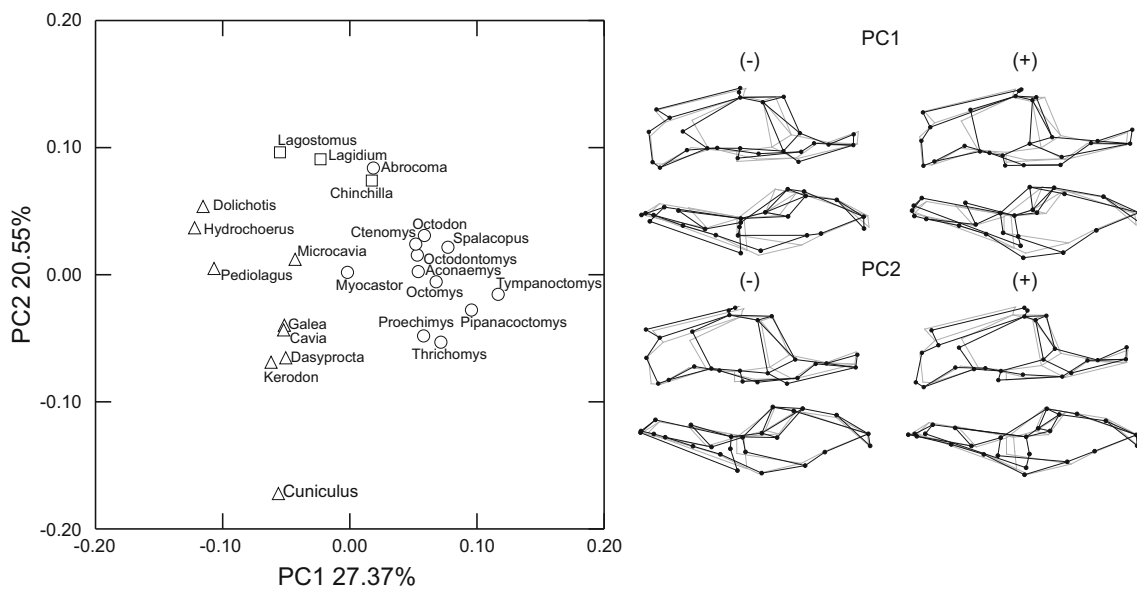


**Fig. 2** Ordination of the 24 caviomorph genera in the morphospace defined by the first two principal components (PCs) of the analysis of shape variation of the face module. Shape changes associated with negative (–) and positive (+) values of both axes are shown as

wireframes: *black dots and lines* indicate shape changes with respect to the mean configuration (indicated with *grey lines*). *Symbols* indicate caviomorph superfamilies: *circles* Octodontoidea, *triangles* Cavoidea, and *squares* Chinchilloidea

Reflecting the distribution of genera along the morphospaces described in the previous section, significant multivariate phylogenetic signal (*Kmult*) for cranial modules and mandible shape datasets was recovered (Table 4).

To examine the patterns of evolutionary shape variation of each module, we performed PCA (one for each cranial module and mandible) using the independent contrasts of shape. Shape changes were similar to that observed in the PCA of the original shape datasets although somewhat more marked in some traits (especially in the face and the mandible; Fig. 6).

The regressions performed between independent contrasts of shape and size hold comparable results to those obtained when analyzing the original data (Table 3; Fig. 7). The main changes related to the increasing size involved the shortening

of the cranial vault, the enlargement of the paroccipital process, the reduction of the size of the auditory bulla, the lengthening of the cranial base, more divergent upper and inferior tooththrows, longer rostral masseteric fossa, the reduction of the size of the coronoid process, more procumbent incisors, and the broadening of the angular process.

**Covariation Patterns Among Cranial Modules and Mandible**

We focused on the first dimension of PLS analyses (i.e. PLS1) since it explained a great proportion of covariance among datasets (Table 5). Cranial vault and base modules showed the largest covariation values, followed by the

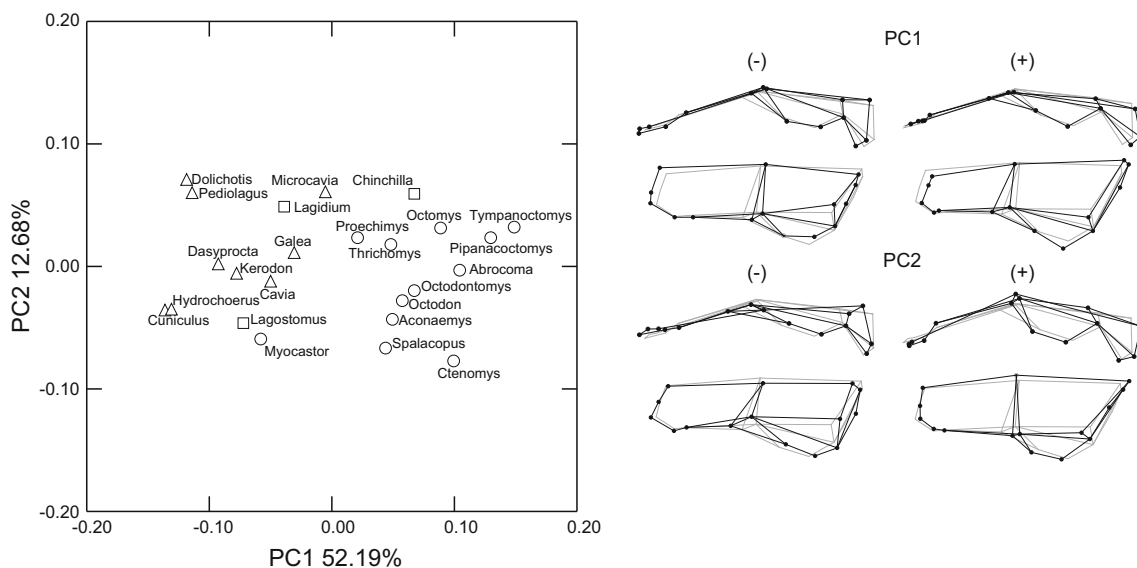


**Fig. 3** Ordination of the 24 caviomorph genera in the morphospace defined by the first two principal components (PCs) of the analysis of shape variation of the cranial vault module. Shape changes associated with negative (–) and positive (+) values of both axes are shown as

wireframes: *black dots and lines* indicate shape changes with respect to the mean configuration (indicated with *grey lines*). *Symbols* indicate caviomorph superfamilies: *circles* Octodontoidea, *triangles* Cavoidea, and *squares* Chinchilloidea

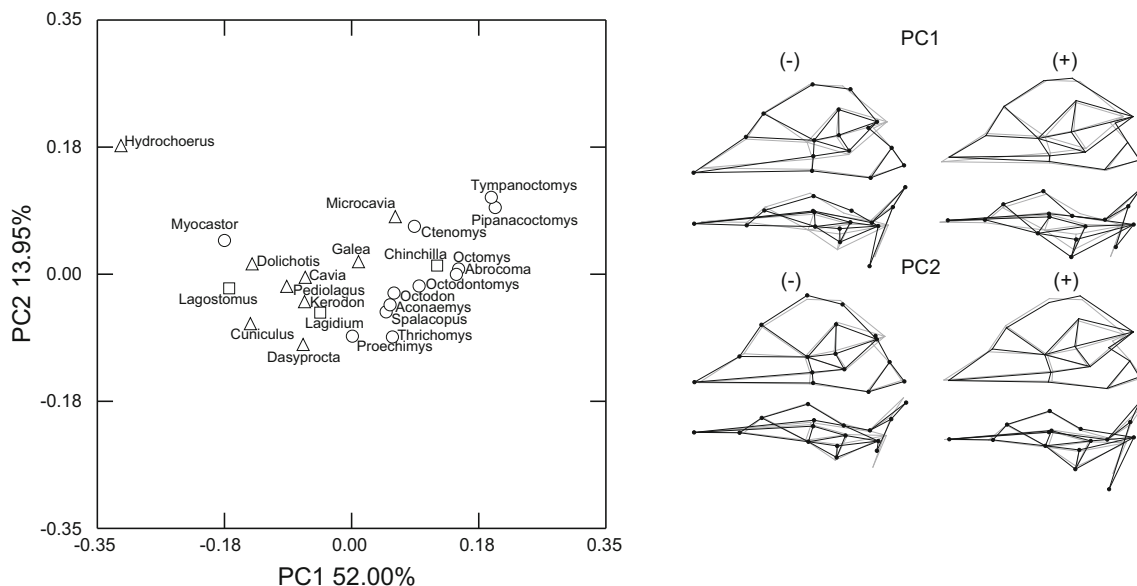


**Fig. 4** Ordination of the 24 caviomorph genera in the morphospace defined by the first two principal components (PCs) of the analysis of shape variation of the cranial base module. Shape changes associated with negative (–) and positive (+) values of both axes are shown as

wireframes: *black dots and lines* indicate shape changes with respect to the mean configuration (indicated with *grey lines*). *Symbols* indicate caviomorph superfamilies: *circles* Octodontoidea, *triangles* Cavoidea, and *squares* Chinchilloidea

covariation between cranial vault and facial modules. The mandible also showed high covariation with the facial module. Overall, the pattern of shape covariation was in agreement with the shape variation detected for each cranial module and the mandible.

*Covariation Between Cranial Vault and Base*

PLS1 accounted for 92.5 % of covariation between datasets, linked to high RV and correlation values (0.85 and 0.95, respectively; Table 5). These values were reflected in the tight

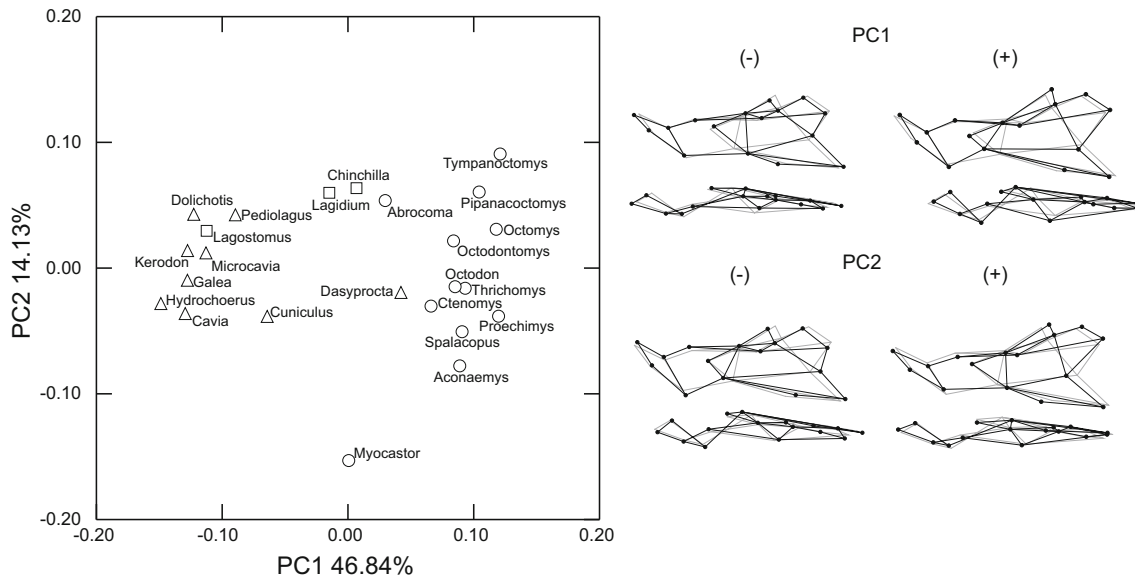


**Fig. 5** Ordination of 24 caviomorph genera analyzed in the morphospace defined by the first two principal components (PCs) of the analysis of mandible shape variation. Shape changes associated with negative (–) and positive (+) values of both axes are shown as

wireframes: *black dots and lines* indicate shape changes with respect to the mean configuration (indicated with *grey lines*). Symbols indicate caviomorph superfamilies: *circles* Octodontoidea, *triangles* Cavoidea, and *squares* Chinchilloidea

**Table 3** Ordinary least squares regressions of shape datasets (i.e. Procrustes coordinates) on size (natural logarithm of centroid size) for the three cranial modules (face, cranial vault and base) and the mandible

	Shape versus size % predicted	<i>P</i>	IC shape versus IC size % predicted	<i>P</i>
Face	21.07	<0.0001	13.62	0.0002
Cranial vault	40.02	<0.0001	21.66	0.0001
Cranial base	43.61	<0.0001	36.89	<0.0001
Mandible	23.61	0.0002	9.50	0.0136

IC, ordinary least squares regressions on phylogenetic independent contrasts of both shape and size

**Table 4** Multivariate *K* statistic (*K*mult) values estimated on the shape datasets (i.e. Procrustes coordinates) of the three cranial modules (face, cranial vault and base) and the mandible

Shape datasets	<i>K</i> mult	<i>P</i>
Face	0.5206	0.003
Cranial vault	0.5644	0.002
Cranial base	0.5383	0.004
Mandible	0.4806	0.014

*P* significance values

distribution of caviomorph genera along this axis (Fig. 8a). Cavioids placed at lower values of PLS1, octodontoids located at positive values (except *Myocastor* that situated near the negative values), and chinchilloids distributed along the PLS1. Shape changes along this axis, from negative to positive values, involved a flatter and wider cranial vault, and an anteriorly tilted occipital plate, covarying with a larger auditory bulla, shorter paroccipital process, and narrower cranial base.

*Covariation Between Cranial Vault and Face*

PLS1 accounted for 81 % of covariation between datasets, linked to high RV and correlation values (0.73 and 0.96,

respectively; Table 5). Cavioids placed at lower values of PLS1 and octodontoids located at positive values (except *Myocastor*); chinchilloids splitted into two groups, with *Lagidium* and *Lagostomus* situated among cavioids and *Chinchilla* among octodontoids. Shape changes along PLS1, from negative to positive values, involved a flatter and wider cranial vault, and an anteriorly tilted occipital plate, covarying with a wider rostrum, a more anterior antorbital bar, a shorter rostral masseteric fossa, and more parallel toothrows (Fig. 8b).

*Covariation Between Cranial Base and Face*

PLS1 accounted for 76 % of covariation between datasets, linked to high correlation value but one of the lowest values of RV (0.90 and 0.65, respectively; Table 5). This could be associated to the more scattered distribution of genera along the PLS1 plot. Anyways, cavioids located at negative values of PLS1, octodontoids placed at positive values (except *Myocastor*) and chinchilloids distributed along the axis. Shape changes along PLS1, from negative

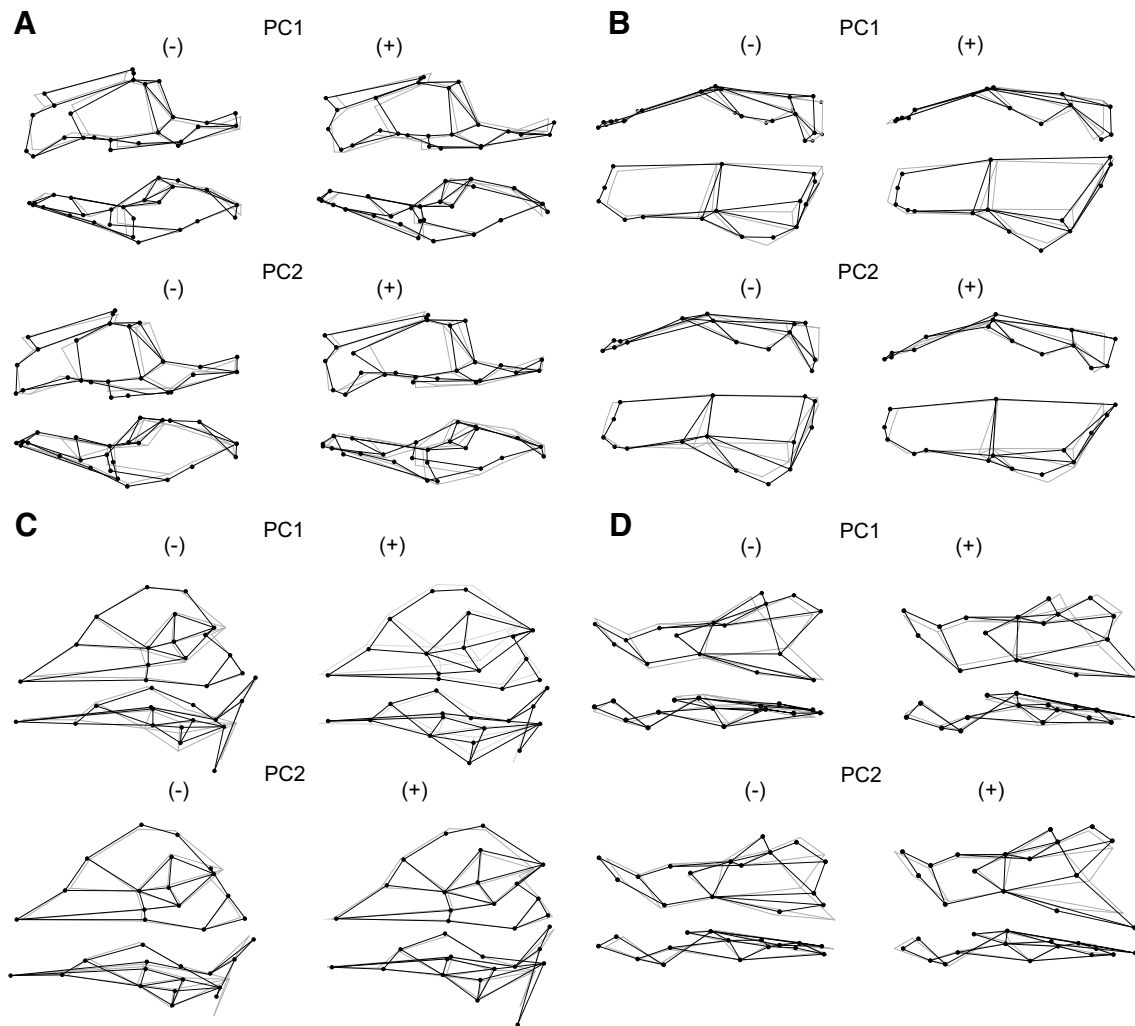


**Fig. 6** Evolutionary shape changes detected through Principal components (PC) analyses of the phylogenetically independent contrasts of the aligned Procrustes coordinates. Shape changes associated with

to positive values, involved a larger auditory bulla, a shorter paroccipital process, and a narrower cranial base, covarying with a wider rostrum, a more anterior antorbital bar, a shorter rostral masseteric fossa, and more parallel toothrows (Fig. 8c).

#### *Covariation Between Mandible and Cranial Modules*

Mandible shape showed high covariation (Table 5) with cranial modules although showed the lowest values for RV, especially for the covariation with cranial base and vault. In the three plots, as occurred with cranial modules, cavioids located at negative values and most octodontoids placed at positive values, while chinchilloids distributed along the axis. Shape changes in the mandible involved a laterally expanded and shorter angular process with its root dorsally placed, and a higher coronoid process (Fig. 8d–f). Cranial modular shape changes involved a wider rostrum, a

negative (–) and positive (+) values of both axes are shown as wireframes: *black dots and lines* indicate shape changes with respect to the mean configuration (indicated with *grey lines*)

more anterior antorbital bar, a shorter rostral masseteric fossa, and more parallel toothrows, in the facial module; a larger auditory bulla and a shorter paroccipital process, for the basicranial module; and an anteriorly tilted occipital plate and a flattened and wider cranial vault (Fig. 8d–f).

The analysis of covariation using the independent contrasts of shape indicated that the patterns observed in the PLS analyses of the original shape datasets were maintained when the phylogenetic structure (PLS on IC of shape) and the effect of size (PLS on the residuals of the regression of IC of shape on IC of size) were considered. However, the RV, covariation, and correlation values were smaller (Table 5). The shape changes associated with the PLS1 of both analyses resulted similar to that observed for the covariation analysis of the original data (Figs. 9 and 10). In all cases, the shape changes were very similar to those related to the allometry and evolutionary allometry analyses.

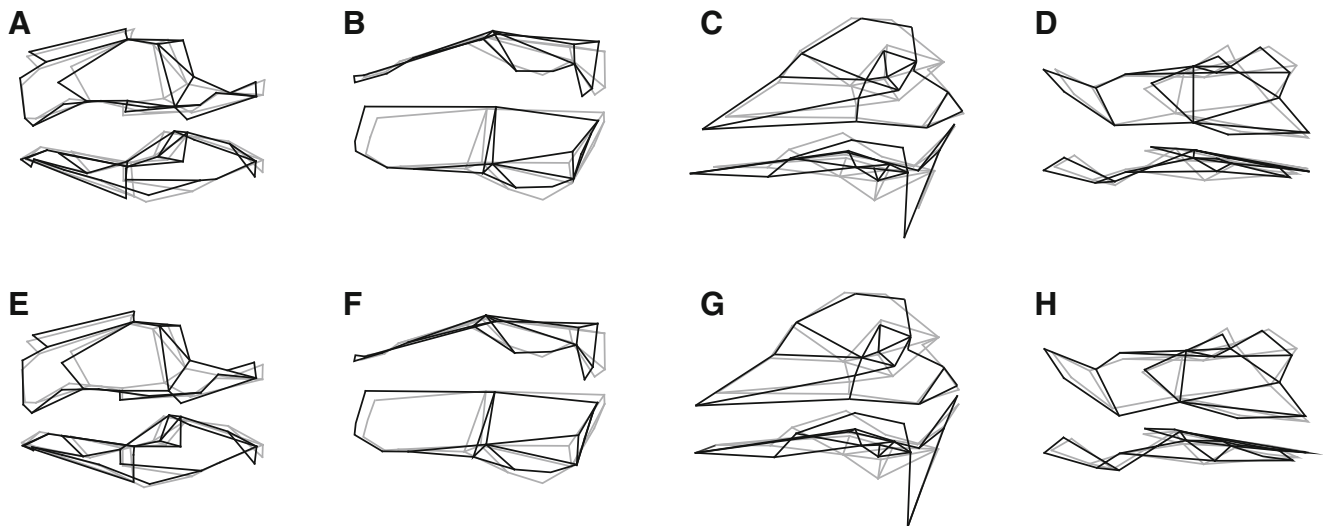


**Fig. 7** Allometric changes in cranial modules and mandible. (A–D) regressions of the aligned Procrustes coordinates on lnCS; (E–H) regressions of the phylogenetically independent contrasts of aligned Procrustes coordinates on the phylogenetically independent contrasts

of lnCS. Shape changes associated with increasing size (per unit) are represented by *black dots and lines*; *grey lines* represent the consensus shape

**Table 5** Results of covariation analyses among cranial modules (face, cranial vault and base) and mandible

	Face	Cranial vault	Cranial base	Mandible
<i>PLS1 shape</i>				
Face		80.90/0.96*	75.91/0.90*	80.42/0.95*
Cranial vault	0.734*		92.50/0.95*	88.00/0.87*
Cranial base	0.645*	0.846*		88.02/0.83**
Mandible	0.708*	0.687*	0.588*	
<i>PLS1 IC shape</i>				
Face		46.02/0.88**	61.83/0.90**	41.46/0.89 <sup>†</sup>
Cranial vault	0.548**		84.55/0.95*	66.40/0.91*
Cranial base	0.576*	0.801*		64.55/0.86**
Mandible	0.556**	0.595*	0.541*	
<i>PLS1 IC residuals</i>				
Face		38.88/0.90*	44.12/0.84 <sup>†</sup>	30.79/0.90**
Cranial vault	0.632*		64.57/0.95*	45.62/0.91*
Cranial base	0.573*	0.784*		43.69/0.88**
Mandible	0.527**	0.530*	0.494**	

Statistics for the first axis (PLS1) of the two-blocks partial least squares analysis are shown. PLS1 shape, analysis on raw shape datasets (i.e. Procrustes coordinates); PLS1 IC shape, analysis on independent contrasts of Procrustes coordinates; PLS1 IC residuals, analysis on the independent contrasts of the residuals of the regression of Procrustes coordinates on size

Below diagonal, RV values; above diagonal, % total covariation/correlation values for PLS1. \*  $\leq 0.0001$ , \*\*  $\leq 0.001$ , <sup>†</sup>  $\leq 0.01$

## Discussion

The mammalian cranium is a complex structure comprised of semi-independent modules with varied morphological integration degrees at ontogenetic (individual) and phylogenetic (evolutionary) levels (e.g. Cheverud 1982; Goswami 2006; Hallgrímsson et al. 2007a). Among caviomorph rodents, cranial modules and the mandible showed high RV values (used as a measure of inter-

modular correlation, ranging between 0.573 and 0.846) which would suggest relatively high levels of evolutionary integration. Although there are no available data on integration patterns at intraspecific levels for caviomorphs, evolutionary changes observed in this work follow similar trends to that observed at ontogenetic levels in other rodents (see Hallgrímsson et al. 2007a; see below). This would suggest the conservation of the mechanisms of development (e.g. Drake and Klingenberg 2010), even across

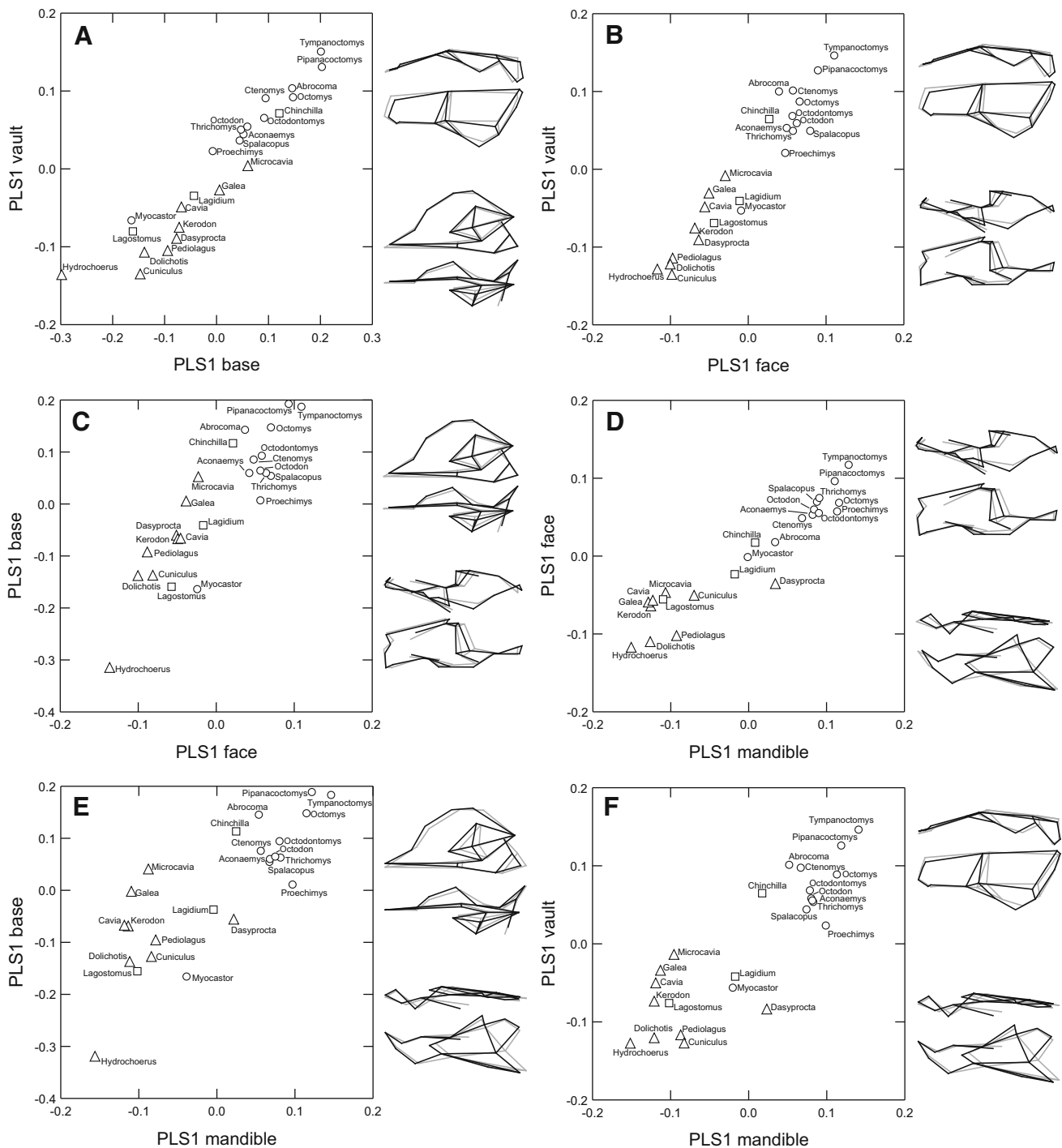


**Fig. 8** Covariation patterns of cranial modules and mandible along the first axis (PLS1) of 2B-PLS analyses carried on the aligned Procrustes coordinates. **a** Cranial vault versus base; **b** cranial vault versus face; **c** cranial base versus face; **d** face versus mandible;

**e** cranial base versus mandible; **f** cranial vault versus mandible. Shape changes toward positive scores of PLS1 are shown as wireframes. Symbols indicate caviomorph superfamilies: circles Octodontoidea, triangles Caviioidea, and squares Chinchilloidea

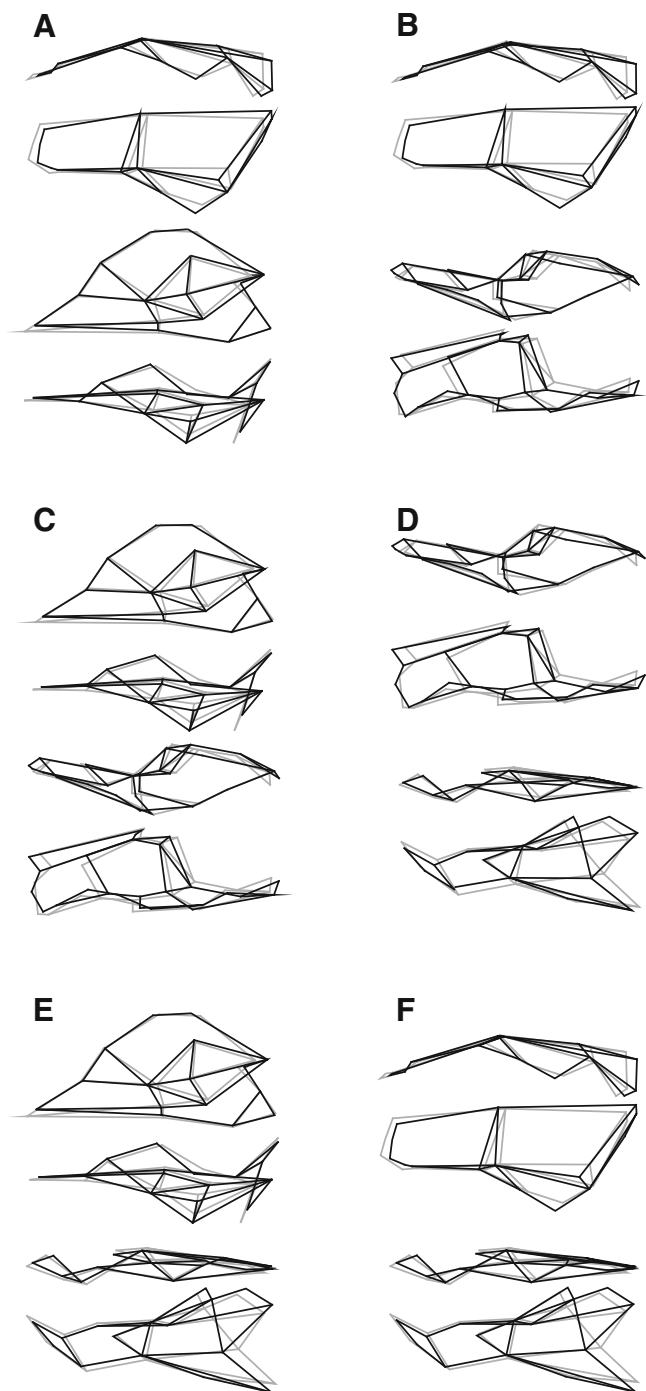
the phylogenetic hierarchy and the ordination of the caviomorph genera along PLS1. Values of  $K_{mult}$  lower than 1 may suggest adaptive evolution as these values would indicate that distantly related species are converging in some traits values, which would be in our case, some

morphological traits, such as an increased bullar size, as discussed below.

Accordingly to the allometric pattern already found for the cranium in an earlier report (38 % of shape explained by size in Álvarez et al. 2013; see also Hautier et al. 2012),

**Fig. 9** Covariation patterns of cranial modules and mandible along the first axis (PLS1) of 2B-PLS analyses carried on the phylogenetically independent contrasts of the aligned Procrustes coordinates.

**a** Cranial vault versus base;  
**b** cranial vault versus face;  
**c** cranial base versus face;  
**d** face versus mandible;  
**e** cranial base versus mandible;  
**f** cranial vault versus mandible.  
 Shape changes toward positive scores of PLS1 are shown as wireframes



a clear trend of association between the shape of skull modules and size was observed, especially for the cranial base and vault. Indeed, smallest caviomorph taxa, such as the octodontids *Tympanoctomys* and *Pipanacoctomys*, display wider and shorter rostra and cranial vault, hypertrophied auditory bullae, shorter paroccipital processes, and robust mandibles with a laterally flared angular process, and high coronoid and condylar processes. All these features change in such a coordinated way that the largest

species, such as the cavioid *Hydrochoerus*, reach “opposite” morphologies, namely, narrower and longer rostrum, narrower cranial vault, reduced auditory bullae, longer paroccipital process, and slender mandibles with angular process non-laterally expanded, and shorter coronoid and condylar processes. Overall, it is assumed that allometry plays a key role in the integration of modules given its global effect on shape (Hallgrímsson et al. 2007b; Klingenberg 2010; Lieberman 2011). However, at least in

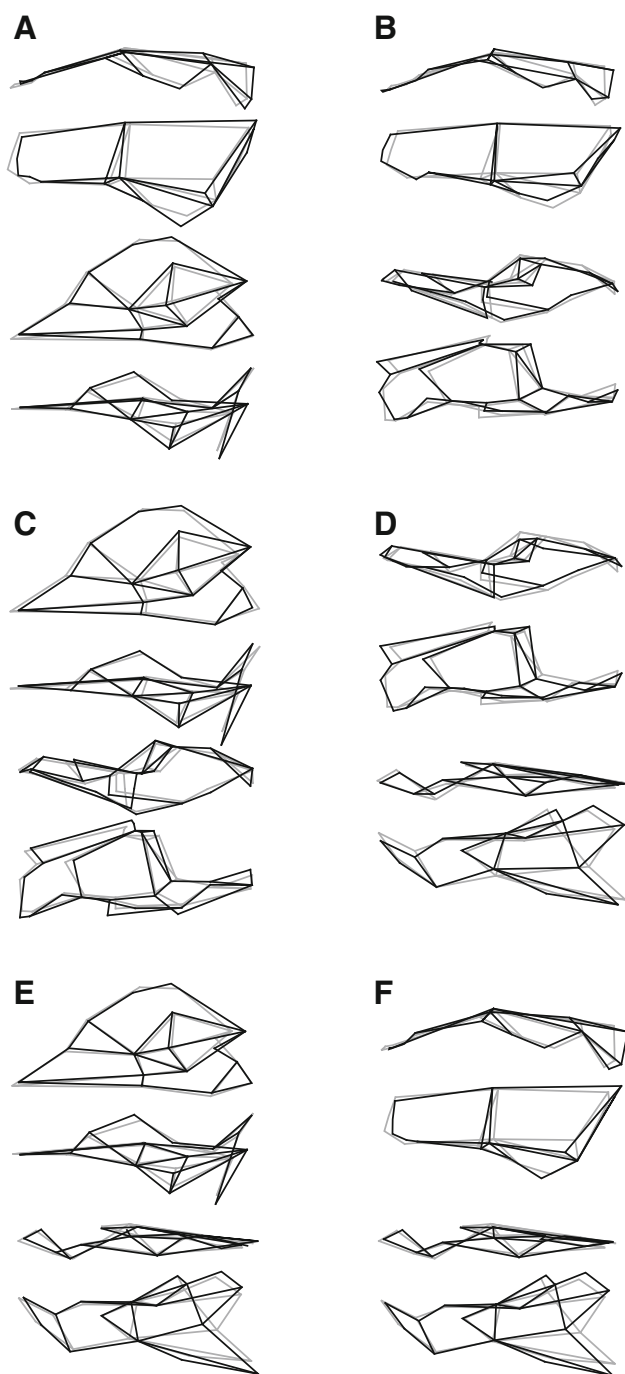


**Fig. 10** Covariation patterns of cranial modules and mandible along the first axis (PLS1) of 2B-PLS analyses carried on the residuals of multivariate regressions between phylogenetically independent contrasts of the aligned Procrustes coordinates on the phylogenetically independent contrasts of the size (lnCS). **a** Cranial vault versus base; **b** cranial vault versus face; **c** cranial base versus face; **d** face versus mandible; **e** cranial base versus mandible; **f** cranial vault versus mandible. Shape changes toward positive scores of PLS1 are shown as wireframes

rodents, this notion contrasts with the relaxed integration found by Wilson and Sánchez-Villagra (2010) in their inclusive allometric analysis spanning all major clades.

Likewise, the maintenance of the integration patterns in caviomorphs after removing allometry suggests that size would not be the only factor contributing to the integration of the cranial units in this group.

Observed covariation among cranial modules and mandible in caviomorphs depicted a pattern similar to that detected for other rodents both among-individual and at ontogenetic scale by Hallgrímsson et al. (2007a). We found the largest covariation between the cranial base and the vault and between the cranial base and the face, a pattern similar to that described by those authors. Moreover, partially consistent with the findings of Hallgrímsson et al. (2007a), one of the main shape changes detected along our datasets involved the coordinated breadth increase of analyzed modules. The overall increase of the cranial base module derived from the widening of the auditory bullae (in coordination with the narrowing of the basicranial bones) may be thought as influencing the integrated development of skull based on the hypothesis that the basicranium is the main integrator of this structure (Lieberman et al. 2000; Hallgrímsson et al. 2007a). In turn, this change may influence the facial and mandible width in order to align the temporomandibular joint to maintain the correct performance of the masticatory apparatus (Hallgrímsson et al. 2007a). This pattern of bullar size differentiation across diverse caviomorph lineages that occupy open and arid environments depicts a clear evolutionary trend that indicates that the development of hypertrophied bullae could be an adaptation to the occupation of this kind of environments (Hafner and Hafner 1988; Ojeda et al. 1999; Verzi 2001).

Alternatively, the adaptive meaning of this pattern has been related to an increasing sensitivity to low-frequency sounds as a strategy to detect predators in open environments (see Schleich and Vassallo 2003; Squarcia et al. 2007). Further, a clear relationship between the morphological variation of the cranial base and vault and size was detected. Considering the direction of the described covariation patterns and the allometric trends, in small species which bear hypertrophied bullae it would be expectable reduced paroccipital processes, shorter rostra and more robust mandible. This may be linked to an ecomorph adapted to arid environments and with likely fossorial habits (as in *Tympanoctomys* or *Ctenomys*) that involve a musculoskeletal reconfiguration associated to higher forces and strains suffered by bone during activities such as burrowing. In contrast, larger species show longer faces (a trend that occurs repeatedly in mammals; Radinsky 1985; Cardini and Polly 2013; Cardini et al. 2015), associated with long paroccipital processes (linked to the development of cervical muscles that hold the head), auditory bullae reduced in size and relatively slender jaws. This ecomorph could be associated to species that inhabit more

humid environments, which generally are not fossorial (except *Lagostomus*), and having a relatively weak masticatory muscles.

The covariation structure of the parts of an adult skull could be thought as a mix of signals left by different sources such as developmental processes and environmental factors acting during the evolution (Hallgrímsson et al. 2007b, 2009). In caviomorphs, the cranio-mandibular morphology would be the outcome of a tight covariation among the modular units of the skull, and its evolution could be driven by several factors, such as allometry and the specializations to environmental niches. Additional studies of ontogenetic series and of well-preserved fossils are required to understand whether the patterns of integration detected in this study occur in the same manner during development and how those patterns have evolved along the history of these rodents.

**Acknowledgments** We thank A.I. Olivares (MLP), D. Flores and S. Lucero (MACN), D. Romero (MPPMa), and R. Ojeda (IADIZA) for providing access to mammalogical material under their care. We are indebted to the anonymous reviewers and B. Hallgrímsson who contributed greatly to improve this manuscript. We want to thank Marcos Ercoli for his help with figure edition. This research is a contribution to Agencia Nacional de Promoción Científica y Tecnológica (ANPCyT) PICT 1150 and PIP 0270 of Consejo Nacional de Investigaciones Científicas y Técnicas grants to D. H. Verzi and ANPCyT PICT 2672 to A. Álvarez.

## References

- Ackermann, R. R., & Cheverud, J. M. (2004). Morphological integration in primate evolution. In M. Pigliucci & K. Preston (Eds.), *Phenotypic integration: Studying the ecology and evolution of complex phenotypes* (pp. 302–319). Oxford: Oxford University Press.
- Adams, D. C. (2014). A generalized K statistic for estimating phylogenetic signal from shape and other high-dimensional multivariate data. *Systematic Biology*, 63(5), 685–697.
- Adams, D. C., & Otarola-Castillo, E. (2013). Geomorph: An R package for the collection and analysis of geometric morphometric shape data. *Methods in Ecology and Evolution*, 4(4), 393–399.
- Álvarez, A., Perez, S. I., & Verzi, D. H. (2011). Ecological and phylogenetic influences on mandible shape variation of South American caviomorph rodents (Rodentia: Hystricomorpha). *Biological Journal of the Linnean Society*, 102(4), 828–837.
- Álvarez, A., Perez, S. I., & Verzi, D. H. (2013). Ecological and phylogenetic dimensions of the cranial shape diversification in South American caviomorph rodents (Rodentia: Hystricomorpha). *Biological Journal of the Linnean Society*, 110(4), 898–913.
- Blomberg, S. P., Garland, J. T., & Ives, A. R. (2003). Testing for phylogenetic signal in comparative data: Behavioral traits are more labile. *Evolution*, 57(4), 717–745.
- Bookstein, F. L., Gunz, P., Mitteroecker, P., Prossinger, H., Schaefer, K., & Seidler, H. (2003). Cranial integration in *Homo*: Singular warps analysis of the midsagittal plane in ontogeny and evolution. *Journal of Human Evolution*, 44(2), 167–187.
- Candela, A. M., & Picasso, M. B. J. (2008). Functional anatomy of the limbs of Erethizontidae (Rodentia: Caviomorpha): Indicators of locomotor behavior in Miocene porcupines. *Journal of Morphology*, 269(5), 552–593.
- Cardini, A., & Elton, S. (2008). Does the skull carry a phylogenetic signal? Evolution and modularity in the guenons. *Biological Journal of the Linnean Society*, 93(4), 813–834.
- Cardini, A., & Polly, P. D. (2013). Larger mammals have longer faces because of size-related constraints on skull form. *Nature Communications*. doi:10.1038/ncomms3458.
- Cardini, A., Polly, P. D., Dawson, R., & Milne, N. (2015). Why the long face? Kangaroos and wallabies follow the same 'rule' of cranial evolutionary allometry (CREA) as placentals. *Evolutionary Biology*. doi:10.1007/s11692-015-9308-9.
- Cheverud, J. M. (1982). Phenotypic, genetic, and environmental morphological integration in the cranium. *Evolution*, 36(3), 499–516.
- Cheverud, J. M. (1996). Developmental integration and the evolution of pleiotropy. *American Zoologist*, 36(1), 44–50.
- Cornette, R., Baylac, M., Souter, T., & Herrel, A. (2013). Does shape co-variation between the skull and the mandible have functional consequences? A 3D approach for a 3D problem. *Journal of Anatomy*, 223(4), 329–336.
- Drake, A. G., & Klingenberg, C. P. (2010). Large-scale diversification of skull shape in domestic dogs: Disparity and modularity. *The American Naturalist*, 175(3), 289–301.
- Eisenberg, J. F., & Redford, K. H. (1999). *Mammals of the Neotropics. Vol. 3: the Central Neotropics—Ecuador, Peru, Bolivia, Brazil*. Chicago: University of Chicago Press.
- Elisamburu, A., & Vizcaino, S. F. (2004). Limb proportions and adaptations in caviomorph rodents (Rodentia: Caviomorpha). *Journal of Zoology London*, 262(2), 145–159.
- Emerson, S. B., & Bramble, D. M. (1993). Scaling, allometry, and skull design. In J. Hanken & B. K. Hall (Eds.), *The skull: Functional and evolutionary mechanisms* (pp. 384–421). Chicago: University of Chicago Press.
- Felsenstein, J. (1985). Phylogenies and the comparative method. *American Naturalist*, 125(1), 1–15.
- Goswami, A. (2006). Cranial modularity shifts during mammalian evolution. *American Naturalist*, 168(2), 270–280.
- Goswami, A., & Polly, P. D. (2010). The influence of modularity on cranial morphological disparity in Carnivora and Primates (Mammalia). *PLoS ONE*, 5(3), e9517.
- Goswami, A., Polly, P. D., Mock, O. B., & Sánchez-Villagra, M. R. (2012). Shape, variance and integration during craniogenesis: Contrasting marsupial and placental mammals. *Journal of Evolutionary Biology*, 25(5), 862–872.
- Goswami, A., Smaers, J., Soligo, C., & Polly, P. D. (2014). The macroevolutionary consequences of phenotypic integration: From development to deep time. *Philosophical Transactions of the Royal Society B*, 369(1649), 20130254.
- Hafner, J. C., & Hafner, M. S. (1988). Heterochrony in rodents. In M. L. McKinney (Ed.), *Heterochrony in evolution: A multidisciplinary approach* (pp. 217–235). New York: Plenum Press.
- Hallgrímsson, B., Jammniczky, H., Young, N. M., Rolian, C., Parsons, T. E., Boughner, J. C., & Marcucio, R. S. (2009). Deciphering the palimpsest: Studying the relationship between morphological integration and phenotypic covariation. *Evolutionary Biology*, 36(4), 355–376.
- Hallgrímsson, B., & Lieberman, D. E. (2008). Mouse models and the evolutionary developmental biology of the skull. *Integrative and Comparative Biology*, 48(3), 373–384.
- Hallgrímsson, B., Lieberman, D. E., Liu, W., Ford-Hutchinson, F. A., & Jirik, F. R. (2007a). Epigenetic interactions and the structure of phenotypic variation in the cranium. *Evolution & Development*, 9(1), 76–91.
- Hallgrímsson, B., Lieberman, D. E., Young, N. M., Parsons, T., & Wat, S. (2007b). Evolution of covariance in the mammalian

- skull. In G. Bock, & J. Goode (Eds.), *Tinkering: The microevolution of development* (pp. 164–187). Chichester: Wiley (Novartis Foundation Symposium 284).
- Hautier, L., Lebrun, R., & Cox, P. G. (2012). Patterns of covariation in the masticatory apparatus of hystricognathous rodents: Implications for evolution and diversification. *Journal of Morphology*, 273(12), 1319–1337.
- Klingenberg, C. P. (2009). Morphometric integration and modularity in configurations of landmarks: Tools for evaluating a priori hypotheses. *Evolution & Development*, 11(4), 405–421.
- Klingenberg, C. P. (2010). Evolution and development of shape: Integrating quantitative approaches. *Nature Reviews Genetics*, 11, 623–635.
- Klingenberg, C. P. (2011). MorphoJ: An integrated software package for geometric morphometrics. *Molecular Ecology Resources*, 11, 353–357.
- Klingenberg, C. P. (2013). Cranial integration and modularity: Insights into evolution and development from morphometric data. *Hystrix*, 24(1), 43–58.
- Klingenberg, C. P., & Marugán-Lobon, J. (2013). Evolutionary covariation in geometric morphometric data: Analyzing integration, modularity, and allometry in a phylogenetic context. *Systematic Biology*, 62(4), 591–610.
- Koyabu, D., Werneburg, I., Morimoto, N., Zollikofer, C. P. E., Forasiepi, A. M., Endo, H., et al. (2014). Mammalian skull heterochrony reveals modular evolution and a link between cranial development and brain size. *Nature Communications*, 5, 3625.
- Lieberman, D. E. (2011). *The evolution of the human head*. Cambridge: Harvard University Press.
- Lieberman, D. E., Pearson, O. M., & Mowbray, K. M. (2000). Basicranial influence on overall cranial shape. *Journal of Human Evolution*, 38(2), 291–315.
- Mares, M. A., & Ojeda, R. A. (1982). Patterns of diversity and adaptation in South American hystricognath rodents. In M. A. Mares & H. H. Genoways (Eds.), *Mammalian biology in South America* (pp. 393–432). Linesville: Special Publication Pymatuning Laboratory of Ecology.
- Marroig, G., & Cheverud, J. M. (2001). A comparison of phenotypic variation and covariation patterns and the role of phylogeny, ecology, and ontogeny during cranial evolution of New World monkeys. *Evolution*, 55(12), 2576–2600.
- Marroig, G., Shirai, L. T., Porto, A., de Oliveira, F. B., & De Conto, V. (2009). The evolution of modularity in the mammalian skull II: Evolutionary consequences. *Evolutionary Biology*, 36(1), 136–148.
- Mitteroecker, P., & Bookstein, F. L. (2007). The conceptual and statistical relationship between modularity and morphological integration. *Systematic Biology*, 56(5), 818–836.
- Mitteroecker, P., & Bookstein, F. L. (2008). The evolutionary role of modularity and integration in the hominoid cranium. *Evolution*, 62(4), 943–958.
- Monteiro, L. R., Bonato, V., & dos Reis, S. F. (2005). Evolutionary integration and morphological diversification in complex morphological structures: Mandible shape divergence in spiny rats (Rodentia, Echimyidae). *Evolution & Development*, 7(5), 429–439.
- Monteiro, L. R., Duarte, L. C., & dos Reis, S. F. (2003). Environmental correlates of geographical variation in skull and mandible shape of the punaré rat *Thrichomys apereoides* (Rodentia: Echimyidae). *Journal of Zoology, London*, 261(1), 47–57.
- Morgan, C. C. (2009). Geometric morphometrics of the scapula of South American caviomorph rodents (Rodentia: Hystricognathi): Form, function and phylogeny. *Mammalian Biology*, 74(6), 497–506.
- Moss, M. L., & Young, R. W. (1960). A functional approach to craniology. *American Journal of Physical Anthropology*, 18(4), 281–291.
- Neaux, D., Guy, F., Gilissen, E., Coudyzer, W., & Ducrocq, S. (2013). Covariation between midline cranial base, lateral basicranium, and face in modern humans and chimpanzees: A 3D geometric morphometric analysis. *The Anatomical Record*, 296(4), 568–579.
- Nowak, R. M. (1991). *Walker's mammals of the world* (5th ed.). Baltimore: Johns Hopkins University Press.
- Ojeda, R. A., Borghi, C. E., Diaz, G. B., Giannoni, S. M., Mares, M. A., & Braun, J. K. (1999). Evolutionary convergence of the highly adapted desert rodent *Tympanoctomys barrerae* (Octodontidae). *Journal of Arid Environments*, 41(4), 443–452.
- Patton, J. L., Pardiñas, U. F. J., & D'Elía, G. (2015). *Mammals of South America, Vol. 2, Rodents*. Chicago: The University of Chicago Press.
- Perez, S. I., Diniz-Filho, J. A. F., Rohlf, F. J., & dos Reis, S. F. (2009). Ecological and evolutionary factors in the morphological diversification of South American spiny rats. *Biological Journal of the Linnean Society*, 98(3), 646–660.
- Porto, A., De Oliveira, F. B., Shirai, L. T., De Conto, V., & Marroig, G. (2009). The evolution of modularity in the mammalian skull I: Morphological integration patterns and magnitudes. *Evolutionary Biology*, 36(1), 118–135.
- R Development Core Team. (2014). *R: A language and environment for statistical computing*. R Foundation for Statistical Computing, Vienna, Austria. <http://www.r-project.org>
- Radinsky, L. B. (1985). Approaches in evolutionary morphology: A search for patterns. *Annual Review in Ecology and Systematics*, 16, 1–14.
- Rinderknecht, A., & Blanco, R. E. (2008). The largest fossil rodent. *Proceedings of the Royal Society B*, 275(1637), 923–928.
- Rohlf, F. J., & Corti, M. (2000). Use of two-block partial least-squares to study covariation in shape. *Systematic Biology*, 49(4), 740–753.
- Rosas, A., & Bastir, M. (2004). Geometric morphometric analysis of allometric variation in the mandibular morphology of the hominids of Atapuerca, Sima de los Huesos site. *The Anatomical Record*, 278(2), 551–560.
- Sánchez-Villagra, M. R., Aguilera, O., & Horovitz, I. (2003). The anatomy of the world's largest extinct rodent. *Science*, 301(5640), 1708–1710.
- Schleich, C. E., & Vassallo, A. I. (2003). Bullar volume in subterranean and surface-dwelling caviomorph rodents. *Journal of Mammalogy*, 84(1), 185–189.
- Squarcia, S. M., Sidorkewicz, N. S., & Casanave, E. B. (2007). The hypertrophy of the tympanic bulla in three species of dasypodids (Mammalia, Xenarthra) from Argentina. *International Journal of Morphology*, 25(3), 597–602.
- Vassallo, A. I., & Verzi, D. H. (2001). Patrones craneanos y modalidades de masticación en roedores caviomorfos (Rodentia, Caviomorpha). *Boletín de la Sociedad de Biología de Concepción, Chile*, 72, 145–151.
- Verzi, D. H. (2001). Phylogenetic position of *Abalosia* and the evolution of the extant Octodontinae (Rodentia, Caviomorpha, Octodontidae). *Acta Theriologica*, 46(3), 243–268.
- Weisbecker, V., & Schmid, S. (2007). Autopodial skeletal diversity in hystricognath rodents: Functional and phylogenetic aspects. *Mammalian Biology*, 72(1), 27–44.
- Willmore, K. E., Young, N. M., & Richtsmeier, J. T. (2007). Phenotypic variability: Its components, measurement and underlying developmental processes. *Evolutionary Biology*, 34, 99–120.
- Wilson, L. A. B., & Sánchez-Villagra, M. R. (2010). Diversity trends and their ontogenetic basis: An exploration of allometric disparity in rodents. *Proceedings of the Royal Society of London B*, 227, 1227–1234.